

Preparation of Chitosan Nanoparticles and Their Application to *Antheraea pernyi* Silk

Yan-Hua Lu,¹ Yu-Yue Chen,² Hong Lin,² Cheng Wang,³ Zhao-Dan Yang¹

¹School of Chemical Engineering and Material Science, Eastern Liaoning University, Dandong 118001, People's Republic of China

²School of Textile and Clothing Engineering, Soochow University, Suzhou 215021, People's Republic of China

³Department of Textile, Zhejiang Textile and Fashion College, Ningbo 315100, People's Republic of China

Received 3 May 2008; accepted 27 December 2009

DOI 10.1002/app.32094

Published online 11 May 2010 in Wiley InterScience (www.interscience.wiley.com).

ABSTRACT: In this study, a chitosan nanoparticle dispersion solution as a novel multifunctional agent was developed to modify *Antheraea pernyi* silk. An ionization gelation methodology with chitosan and sodium tripolyphosphate (STPP) was used to prepare the chitosan nanoparticle solution, and then, Fourier transform infrared spectra, laser particle size analysis, and transmission electron microscopy (TEM) were used to characterize the structure and size distribution of the chitosan nanoparticles. The peaks at 3390.7, 1633.7, 1538.2, and 1258.1 cm^{-1} revealed the reaction between the chitosan and STPP molecules in the chitosan nanoparticles. The average size of the nanoparticles in the aqueous dispersion solution was approximately 20 nm. TEM images clearly showed the

round spherical morphology and the distribution of the particles in the solid state. The obtained chitosan nanoparticle dispersion solution was then applied to treat silk filaments and fabric. The results indicate that the surface of the chitosan-nanoparticle-treated *A. pernyi* silk fiber was rougher than that of the chitosan-treated and untreated ones, and a higher specific surface was achieved. In addition, the antibacterial activity, breaking strength, and wrinkle-resistance properties of the chitosan-nanoparticle-treated *A. pernyi* silk fabric were also enhanced. © 2010 Wiley Periodicals, Inc. *J Appl Polym Sci* 117: 3362–3369, 2010

Key words: biopolymers; functionalization of polymers; mechanical properties; nanotechnology

INTRODUCTION

Antheraea pernyi silk, a kind of wild silk, is an excellent clothing material with an inherent elegant sheen, soft and smooth hand, beautiful appearance, moisture absorption, sweat exclusion, and affinity to human skin. However, there are some disadvantages of the silk fabric, including a poor wrinkle-recovery performance and limited functions in comparison with other fabrics. In past decades, some researchers attempted to modify the silk fabric by treating it with traditional chemical agents.^{1–5} These studies can help with development to some extent, which can promote the research in this field, but there still exist problems in poor feel, low water-vapor permeability, and poor skin affinity. To improve these properties these days, some biomaterials, including chitosan

and natural silk fibroin, have been applied to textiles,^{6,7} which has provided an approach to the development of a kind of novel functional textile.

Chitosan, obtained from the shells of crabs, shrimp, and other crustaceans, is the second most abundant polysaccharide, with special characteristics of nontoxicity, biodegradability, and biocompatibility. It has been widely applied in the medical, papermaking, and food-processing industries.^{8,9} As the safest and most effective antibacterial agent, chitosan has also been applied to the improvement of the mechanical properties and dyeability of natural fabrics.^{10–14} Recently, chitosan nanoparticles have been studied and applied as drug carriers in the genetic transmission field.^{15,16}

In this study, a chitosan nanoparticle dispersion solution was prepared by the ionization gelation methodology and then applied to modify *A. pernyi* silk fabric. The structure, size distribution, and morphology of the chitosan nanoparticles were investigated. Also, the effect of 1,2,3,4-butane tetracarboxylic acid (BTCA), sodium hypophosphite (SHP), and chitosan concentrations on the mechanical properties, whiteness index, wrinkle-resistance properties, and antibacterial properties of *A. pernyi* silk filaments or fabric were examined. The purpose of this study

Correspondence to: Y.-H. Lu (yanhualu@yaho.com.cn).

Contract grant sponsor: Education Department Funds of Liaoning Province; contract grant number: 20060301.

Contract grant sponsor: Science and Technology Foundation Project of Dandong; contract grant number: 07143.

was to provide a sound basis for the further functional exploration of *A. pernyi* silk.

EXPERIMENTAL

Materials

Chitosan (viscosity-average molecular weight = 20,000, degree of deacetylation = 92.0%) was prepared by the degradation of a commercial chitosan (viscosity average molecular weight = 240,000, degree of deacetylation = 92.0%) according to Shin et al.¹⁷

The *A. pernyi* silk filaments and fabric (type 5023, 100 g/m²) used in the experiment were carried out on degummed silk fabric (degumming rate = 13.0%), which was purchased from Liaoning Tussah Silk Institute Co., Ltd. (Dangdong, China).

The BTCA, SHP, sorbitan monooleate (Span-80), and sodium tripolyphosphate (STPP) used in this experiment were chemical pure agents. Gram-positive *Staphylococcus aureus* (ATCC 6538) was used as the test microorganism.

Preparation of the aqueous treatment solution

The aqueous treatment solution, containing BTCA, SHP, Span-80, and chitosan nanoparticles, was prepared by an ionization gelation method.¹⁷ Chitosan was first dissolved in a BTCA and SHP aqueous solution with 0.05 wt % Span-80. Then, an aqueous solution containing 0.5 wt % STPP was dropped into the previous solution at 40°C with stirring. The size distribution of the chitosan nanoparticles in the aqueous dispersion solution was controlled at about 20 nm by adjustment of the concentration of STPP with high performance particle sizer (Model HPPS 5001, Malvern Instruments Ltd., Malvern, UK) monitoring. Aqueous treatment solutions containing BTCA and SHP only as well as a chitosan precursor were prepared by the dissolution of only BTCA, SHP, and chitosan at 40°C with stirring.

The viscosity-average molecular weight of chitosan was selected as 20,000 in this experiment because small chitosan molecules could provide some special properties, such as antibacterial activity, moisture absorption, and moisture-retention abilities.¹⁸ BTCA was used as the crosslinker between *A. pernyi* silk fibroin and chitosan by the catalysis of SHP, and its aqueous acidic solution acted as the solvent of chitosan and was also used as the dispersion medium of the chitosan nanoparticles. Span-80 in the solution helped to disperse the chitosan nanoparticles as a dispersant.

Treatment of the *A. pernyi* silk filaments and fabric

A. pernyi silk samples were immersed in the aqueous treatment solution at 40°C for 30 min at a liquor

ratio of 1 : 50 padded at a 90% wet pick-up. After these processes, the samples were dried at 80°C for 5 min and then cured in a laboratory oven at 160°C for 3 min.¹⁹ The treated samples were then washed with tap water and washed further in deionized water in an ultrasonic cleaner for 5 min to remove the unfixed materials. Finally, the samples were dried at 80°C in a laboratory oven for 2 h.

For the combination treatment of BTCA, SHP, and chitosan nanoparticles of the *A. pernyi* silk samples, the finishing variables were as follows: the BTCA and SHP concentrations ranged from 0 to 5 wt %, and the chitosan concentrations ranged from 0 to 1.2 wt %, respectively. As for the BTCA and SHP only treatment of *A. pernyi* silk samples, the treatment solution formula was based on the formula of the combination treatment of BTCA, SHP, and chitosan nanoparticles, but the chitosan concentration selected was 0.

Analysis of the particle size distribution

The average diameter and size distribution of the chitosan nanoparticles in the dispersion aqueous solution were measured with a Malvern HPPS 5001 particle size analyzer at 40°C, which corresponded to the temperature of the *A. pernyi* silk filament and fabric treatment.

Images of the nanoparticles and *A. pernyi* silk fiber morphology

To determine the morphology and size distribution of chitosan nanoparticles, a drop of sample solution was placed onto a 300-mesh copper grid coated with carbon. Approximately 2 min after deposition, the grid was tapped with filter paper to remove surface water and air-dried. Nanostructures of the chitosan particles were observed with a transmission electron microscope (Hitachi H-60, Hitachi Instruments Service Co. Ltd, Tokyo, Japan) at an accelerating voltage of 200 kV.

The morphology of the *A. pernyi* silk fiber before and after treatment was evaluated by scanning electron microscopy (SEM; Hitachi H-600, 120 kV, 0.26-nm point resolution). The samples were mounted and gold-sputtered to give the samples electronic conductivity *in vacuo* before observation.

Fourier transform infrared (FTIR) spectra of the chitosan nanoparticles

Infrared spectra of the chitosan nanoparticles and chitosan were recorded on a Nicolet 5700 FTIR spectrophotometer (Thermo Electron Corp., Waltham, MA) with KBr disks. The measurements were performed at 20°C and a relative humidity of 65%.

TABLE I
Effect of the BTCA Concentration on the Properties of the *A. pernyi* Silk Filaments and Fabric

BTCA concentration (%)	Breaking strength (cN/dtex)	Wrinkle-recovery angle: $W + F$ (°)	Whiteness index (%)	Bacterial reduction (%)	
				Before 20 launderings	After 20 launderings
0	2.10	197.4	68.5	57.9	23.7
1	2.16	215.1	63.6	94.4	87.6
2	2.20	246.8	62.1	94.0	90.1
3	2.18	259.3	61.7	93.2	89.4
4	2.14	267.5	60.9	92.3	87.7
5	2.08	271.9	60.6	92.0	87.1

W, Warp; F, Fill/Weft.

Mechanical properties of the *A. pernyi* silk filaments

The samples were put in the room (20°C, relative humidity = 65%) for 48 h before measurement. The breaking strength of the *A. pernyi* silk filaments (before and after treatment) was determined by an Instron 3365 universal testing machine (model 3365, Instron Corp., Canton, MA). An average result was obtained from 10 samples.

Wrinkle-resistant properties of the *A. pernyi* silk fabrics

The dry wrinkle-recovery angles of the *A. pernyi* silk fabrics (before and after treatment) were evaluated by a YG541A wrinkle-recovery tester (Darong Standard Textile Apparatus Co., Ltd., Wenzhou, China) according to AATCC test method 66-1998. We obtained the results by averaging 10 wrap and 10 weft samples, respectively.

Whiteness index of the *A. pernyi* silk fabrics

The whiteness index was measured by a ColorEye 7000A spectrophotometer (Macbeth Co., New York, NY) according to AATCC test method 110-1995. Each *A. pernyi* silk fabric sample was folded into eight layers, and we obtained the results by averaging 10 samples.

Antibacterial activity of the *A. pernyi* silk fabrics

The antibacterial activity of the *A. pernyi* silk fabrics before and after treatment was evaluated quantitatively by the shake flask method.²⁰ This method is specially designed for specimens treated with nonreleasing antibacterial agents under dynamic contact conditions. *S. aureus* (ATCC 6538), a Gram-positive bacterium commonly found on the human body, was chosen as the tested bacterium. A typical procedure was as follows: 1 ± 0.1 g of sample fabric, cut into small pieces approximately 0.5 × 0.5 cm², was dipped into a flask containing 50 mL of a 0.5 mM monopotassium phosphate culture solution with a cell concentration of 1.0–1.5 × 10⁴/mL. The flask was then shaken at 250 rpm on a rotary shaker at

37°C for 1 h. Before and after shaking, 1 mL of the test solution was extracted, diluted, and spread onto an agar plate. After incubation at 37°C for 24 h, the number of colonies formed on the agar plate was counted, and the number of live bacterial cells in the flask before and after shaking was calculated. The antibacterial efficacy was determined on the basis of duplicated test results. The percentage of bacterial reduction (*R*) was calculated according to the following equation:

$$R = \frac{B - A}{B} \times 100\%$$

where *B* and *A* are the numbers of live bacterial cells in the flask before and after, respectively, 1 h of shaking.

RESULTS AND DISCUSSION

Treatment of the *A. pernyi* silk filaments and fabrics

In the experiment, the effect of BTCA, SHP, and chitosan concentration on the properties of the *A. pernyi* silk filaments and fabrics treated with the nanochitosan dispersion solution were examined.

Effect of the BTCA concentration on the properties of *A. pernyi* silk treated with 1 wt % chitosan, 2 wt % SHP, 0.05 wt % Span-80, and 0.5 wt % STTP

The effect of the BTCA concentration on the properties of the *A. pernyi* silk is shown in Table I, which indicates that the breaking strength of the treated *A. pernyi* silk filaments changed slightly when the BTCA concentration ranged from 1 to 3 wt % but was more than that of the untreated *A. pernyi* silk filaments. The wrinkle-recovery angle increased for the crosslinking reaction among *A. pernyi* silk fibroin, BTCA, and chitosan when the BTCA concentration was increased. However, the whiteness index decreased with increasing BTCA concentration.

Before 20 launderings, the bacterial reduction of the treated *A. pernyi* silk decreased with increasing BTCA concentration and was obviously greater than that of the untreated one. The main reason was that

TABLE II
Effect of the SHP Concentration on the Properties of the *A. pernyi* Silk Filaments and Fabric

SHP concentration (%)	Breaking strength (cN/dtex)	Wrinkle-recovery angle: W + F (°)	Whiteness index (%)	Bacterial reduction (%)	
				Before 20 launderings	After 20 launderings
0	2.10	198.2	68.7	57.4	30.1
1	2.13	217.7	65.3	95.0	85.5
2	2.19	240.3	64.8	94.7	89.8
3	2.20	250.1	62.0	94.6	90.4
4	2.19	251.5	61.6	93.2	88.7
5	2.17	252.9	61.1	92.8	87.8

W, Warp; F, Fill/Weft.

—NH₂ in the chitosan molecules provided an antibacterial function, and its amount decreased with the occurrence of the crosslinking reaction between a part of —NH₂ in chitosan and —COOH in the BTCA molecules. As a result, the antibacterial properties of the *A. pernyi* silk declined. However, after 20 launderings, the bacterial reduction increased when the BTCA concentration ranged from 0 to 2 wt % and decreased slightly when the BTCA concentration was greater than 2 wt %. We concluded that the increased bacterial reduction after 20 launderings was due to the crosslinking reaction, which limited the loss of chitosan in the process of the launderings, and the slightly decreased bacterial reduction was attributed to the decline of —NH₂ in chitosan with the reaction between —COOH in the BTCA molecules.

On the basis of an overall consideration of the various properties of the treated *A. pernyi* silk, especially the antibacterial properties, the BTCA concentration selected was 2 wt %.

Effect of the SHP concentration on the properties of *A. pernyi* silk treated with 1 wt % chitosan, 2 wt % BTCA, 0.05 wt % Span-80, and 0.5 wt % STTP

As shown in Table II, the breaking strength of the treated *A. pernyi* silk filaments changed slightly when the SHP concentration ranged from 2 to 5 wt % but was greater than that of the untreated sample. The wrinkle-recovery angle increased greatly when

the SHP concentration increased from 1 to 3 wt % and increased slightly when the SHP concentration was greater than 3 wt %. The increased breaking strength and wrinkle-recovery angle were attributed to the crosslinking reaction by the catalysis of SHP in the reactions among BTCA, chitosan, and *A. pernyi* silk. The whiteness index decreased a little compared with that of the effect of the BTCA concentration on the *A. pernyi* silk (Table I) when the SHP concentration was increased. The decreased whiteness index was due to the side reaction between BTCA and *A. pernyi* silk and the color of chitosan itself.

Before 20 launderings, the bacterial reduction decreased when the SHP concentration ranged from 1 to 5 wt % and was greater than that of the untreated *A. pernyi* silk filaments. The reason was that —NH₂ in the chitosan molecules decreased with the occurrence of the crosslinking reaction between a part of —NH₂ in chitosan and —COOH in the BTCA molecules for the catalysis of SHP, and as a result, the antibacterial properties declined with increasing SHP concentration. However, the bacterial reduction after 20 launderings increased when the SHP concentration was less than 3 wt % and decreased slightly when the SHP concentration was greater than 3 wt %. The reason was that SHP acted as a catalyst in favor of the reaction of BTCA, chitosan, and *A. pernyi* silk fibroin, which limited the loss of chitosan nanoparticles in the process of washing. Because of the effect on the overall properties of *A.*

TABLE III
Effect of the Chitosan Concentration on the Properties of the *A. pernyi* Silk Filaments and Fabric

Chitosan concentration (%)	Breaking strength (cN/dtex)	Wrinkle-recovery angle: W + F (°)	Whiteness index (%)	Bacterial reduction (%)	
				Before 20 launderings	After 20 launderings
0	2.07	241.2	66.7	30.4	28.1
0.2	2.13	247.7	65.3	78.5	71.6
0.4	2.16	248.3	64.4	83.8	77.4
0.6	2.17	252.1	63.8	88.3	83.2
0.8	2.17	255.6	62.7	92.3	88.5
1.0	2.15	256.9	61.9	94.7	90.5
1.2	2.12	257.6	60.6	94.9	90.6

W, Warp; F, Fill/Weft.

pernyi silk, especially the antibacterial properties, the SHP concentration selected was 3 wt %.

Effect of the chitosan concentration on the properties of *A. pernyi* silk treated with 2 wt % BTCA, 3 wt % SHP, 0.05 wt % Span-80, and 0.5 wt % STTP

The effect of the BTCA, SHP (without chitosan), and chitosan concentrations on the *A. pernyi* silk properties are shown in Table III. It was obvious that the breaking strength and wrinkle-recovery angles of the *A. pernyi* silk were enhanced after treatment with the nanochitosan dispersion treatment solution. However, for whiteness index retention, a reduction was obtained compared to that of the *A. pernyi* silk fabrics treated with BTCA and SHP only. The increments of breaking strength and wrinkle-recovery angle of the *A. pernyi* silk samples were based on the crosslinking reactions among molecules of BTCA, chitosan, and *A. pernyi* silk fibroin in the process of the chitosan nanoparticle dispersion solution treatment, which limited the movement of macromolecular chains in the amorphous field of the *A. pernyi* silk fiber.²¹ On the other hand, chitosan nanoparticles in the treatment solution may have entered into and filled the voids of the *A. pernyi* silk fiber in the process of wet treatment.¹⁸ The decrement of the whiteness index retention was based on the two following reasons: one was the color of chitosan itself, and the other was the side reactions of BTCA. However, the *A. pernyi* silk itself also had a natural light yellow color, so yellowing was not a main problem in the experiment.

The antibacterial activity of the treated *A. pernyi* silk fabric before and after 20 launderings increased with increasing chitosan concentration, but only a slight increase in the antibacterial activity was obtained when the concentration of chitosan was more than 1 wt %. Because of the hand and white-

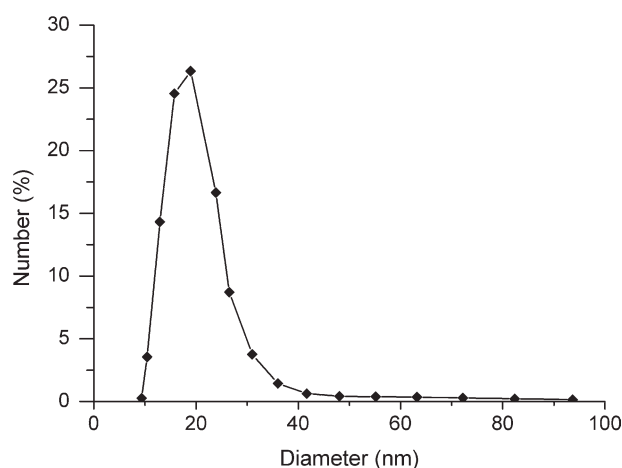


Figure 1 Size and distribution of the chitosan nanoparticles in the dispersion solution.

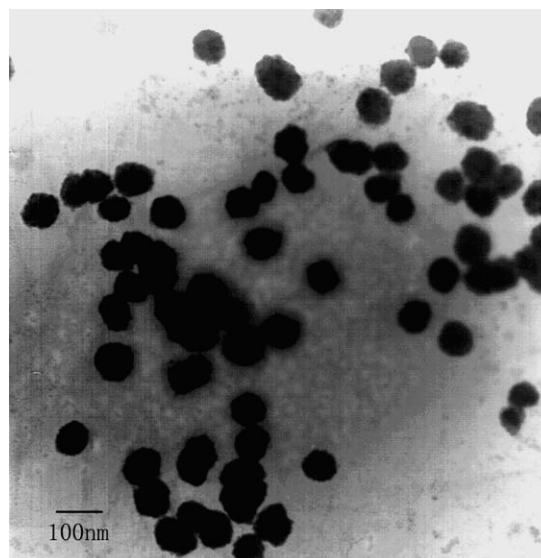


Figure 2 TEM micrograph of the chitosan nanoparticles.

ness index of the *A. pernyi* silk fabric, the chitosan concentration in the chitosan nanoparticle dispersion solution selected was 1 wt %.

According to the effects of the BTCA, SHP, and chitosan concentrations on the breaking strength, wrinkle-recovery angle, and especially, the antibacterial properties, the optimum formulation was selected as follows: 2 wt % BTCA, 3 wt % SHP, 1 wt % chitosan, and 0.05 wt % Span-80. A concentration of 0.5 wt % STTP was used to prepare the nanochitosan dispersion treatment solution, and the size of the chitosan nanoparticles was controlled at about 20 nm by adjustment of the amount of STTP.

On the basis of the previous formulation, the prepared chitosan nanoparticles was characterized, and the properties of the *A. pernyi* silk treated with chitosan nanoparticles were also determined and

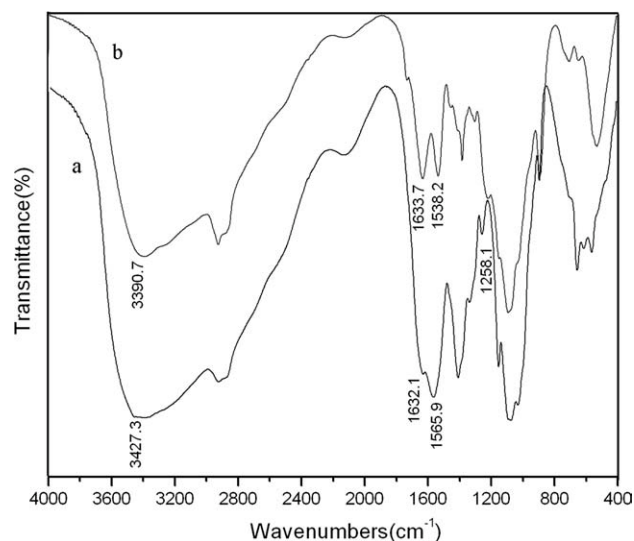
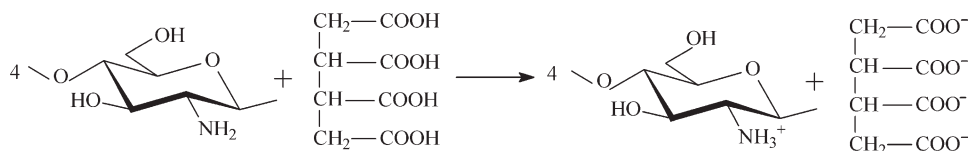


Figure 3 FTIR spectra: (a) chitosan and (b) nanochitosan.



Scheme 1 Reaction between chitosan and BTCA.

compared to that of the chitosan-precursor-treated and untreated ones.

Analysis of the chitosan nanoparticles

In this experiment, the size distribution of the chitosan nanoparticles in the aqueous dispersion solution was analyzed with an HPPS particle size analyzer. The size distribution and morphological characterizations of the chitosan nanoparticles in the solid state were evaluated with transmission electron microscopy (TEM). The results are shown in Figures 1 and 2.

Figure 1 shows that the primary size range of the chitosan nanoparticles in the dispersion solution was 15–40 nm, and the average diameter and polydispersity index of the particles were 20.8 nm and 0.43, respectively, which indicated that chitosan nanoparticles were dispersed perfectly and that the distribution of the nanoparticles was relatively narrow.

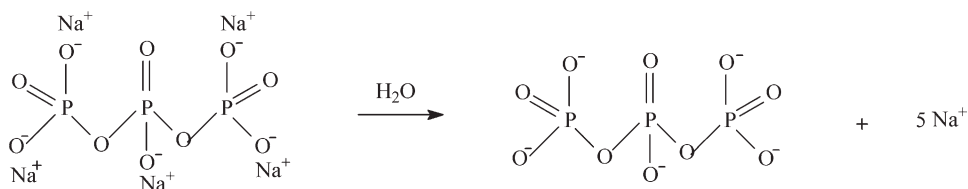
The TEM micrographs of the chitosan nanoparticles in Figure 2 illustrate that the chitosan nanoparticles in the solid state were nearly spherical in shape and had a near uniform particle size distribution. This result was accordant with previous research on chitosan nanoparticles.^{22,23} The average size of almost all of the particles was less than 100 nm; however, the average diameter was 83.6 nm, obviously larger than that tested by the HPPS particle size analyzer. The reason for the difference was that the obtained diameters by TEM were not that of single chitosan primary nanoparticles but that of the secondary particles aggregated from several particles whose sizes ranged from 15 to 40 nm. In the preparation process of the chitosan nanoparticles, the emulsion phenomenon was observed when the solution of chitosan nanoparticles was put above 2 h, which was in accordance with the results obtained by TEM. The reason was as follows: first, the nano-

particle itself contained an amount of surface energy and tended to aggregate spontaneously,²⁴ which resulted in a system of chitosan nanoparticles that was not stable. Second, the HPPS particle size analyzer was used in the aqueous solution, while the TEM observation was performed in the solid state after water vaporization. The aggregation chance of the chitosan nanoparticles increased with water vaporization in the preparation the sample for TEM.

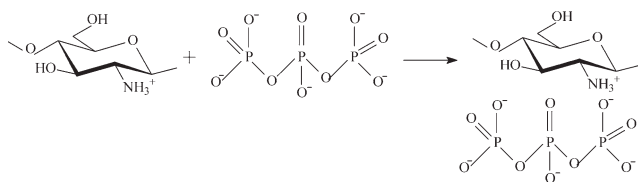
The FTIR spectra of chitosan and nanochitosan are shown in Figure 3. A broad peak of 3427.3 cm^{-1} in the chitosan sample was obtained. However, for the nanochitosan, the peak at 3427.3 cm^{-1} shifted to 3390.7 cm^{-1} , which indicated that the formation of the intermolecular bonds (H–N \cdots O–H, H–O \cdots H–O, and P–O \cdots H–O in chitosan chains) and intramolecular hydrogen bonds²⁵ (H–N \cdots O–H, H–O \cdots H–O, and P–O \cdots H–O among chitosan chains) in the chitosan nanoparticles. The shoulder peak at 1632.1 cm^{-1} shifted to a sharp peak at 1633.7 cm^{-1} ($\nu_{\text{C}=\text{O}}$ of chitosan linked with STTP), and the intensity of peak also obviously increased, whereas the peak at 1565.9 cm^{-1} ($\delta_{\text{N}-\text{H}}$ of chitosan) disappeared, and a new peak at 1538.2 cm^{-1} ($\delta_{\text{N}-\text{H}}$ of chitosan linked with STTP) appeared. The results indicate that an adsorption reaction between the phosphate anion in STPP and $-\text{NH}_3^+$ of chitosan occurred. In addition, the peak of dissociative hydroxyl at 1258.1 cm^{-1} obviously became weak after chitosan reacted with STPP, which indicated the formation of chitosan nanoparticles. The reaction mechanism is shown in Schemes 1–3.

Morphology of the *A. pernyi* silk fiber

The surface characteristics of the untreated chitosan precursor and chitosan-nanoparticle-treated *A. pernyi* silk fiber were investigated by SEM (Fig. 4). The images showed an obviously different morphology



Scheme 2 Reaction of STPP in an aqueous solution.



Scheme 3 Reaction between chitosan and SPP.

among the untreated chitosan precursor and the chitosan-nanoparticle-solution-treated silk fiber. The surface of the untreated silk fiber was smooth. However, after treatment by chitosan nanoparticles, the surface of the silk fiber became relatively rough, and the surface of the silk fiber treated by the chitosan nanoparticles was rougher than that treated by the chitosan precursor, and many cracks appeared. This indicated that the specific surface area of the chitosan-nanoparticle-treated silk fiber was larger than that of the untreated and chitosan-precursor-treated ones. As a result, the chitosan-nanoparticle-treated silk fiber had a greater ability to adsorb chemicals in the subsequent wet treatment process. In addition, the nanoparticles could be obviously observed on the surface of silk fiber, and the sizes of little individual particles were larger than 100 nm.

Antibacterial activity of the *A. pernyi* silk fabrics

In this experiment, *A. pernyi* silk fabrics were treated with the precursor chitosan aqueous solution, and the nanochitosan dispersion solution contained BTCA and SHP. The bacterial reductions against *S. aureus* before and after 20 launderings are shown in Figure 5.

It was indicated that the untreated *A. pernyi* silk fabric silk fiber itself provided definite antibacterial properties of over 20% bacterial reduction for the

-NH_2 in fibroin of *A. pernyi* silk, and the bacterial reduction of the untreated sample increased a little after 20 launderings. The reason may have been the lost of residual sericin, which surrounded the silk fiber after 20 launderings. Also, the bacterial reduction of the chitosan-precursor-treated sample before and after 20 launderings was greater than that of the untreated sample. This was attributed to the relatively high amount of chitosan on the *A. pernyi* silk fabric after the chitosan precursor treatment, which may have enhanced the antibacterial activity, in which a large amount of protonated chitosan may have come into contact with the bacterial cell surface and prevented the leakage of intracellular components.²⁶ Furthermore, the bacterial reduction of the nanochitosan-dispersion-solution-treated silk sample was greater than that of the chitosan-precursor-treated one before and after 20 launderings; this could have been because of the increased specific surface area of the nanochitosan-treated *A. pernyi* silk fiber in comparison to that of the chitosan-precursor-treated and untreated silk fibers (shown in Fig. 5). As a result, the contact area between the treated silk fabric and bacteria increased, and more bacteria could be killed.

CONCLUSIONS

A chitosan nanoparticle dispersion solution was prepared by an ionization gelation methodology. Chitosan nanoparticles with an average size of 20.8 nm dispersed homogeneously in the obtained treatment solution. The antibacterial efficacy of the *A. pernyi* silk fabric treated with the chitosan nanoparticle dispersion solution was better than that of the fabric treated with chitosan precursor and significantly better than that of the untreated fabric. The bacterial reductions of the *A. pernyi* silk fabric treated with

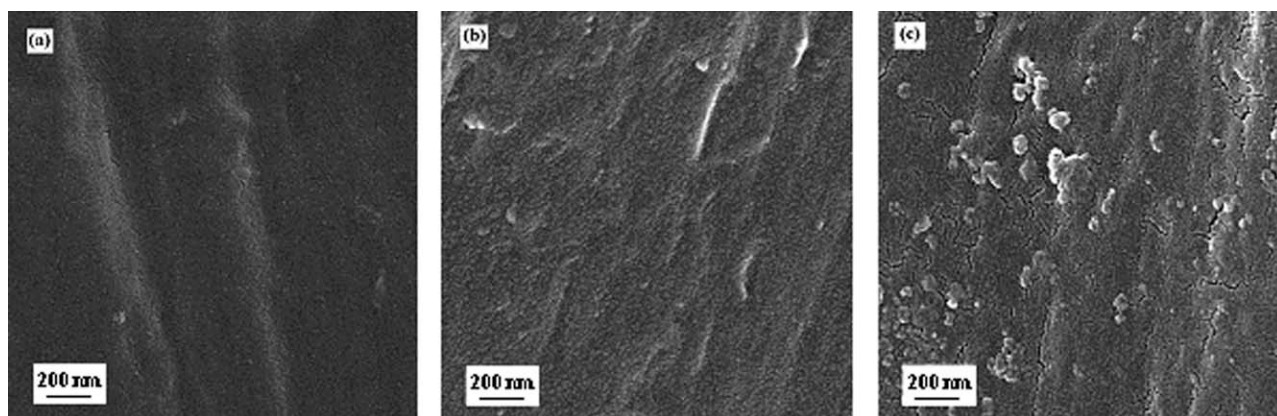


Figure 4 SEM micrographs of *A. pernyi* silk fiber: (a) untreated fiber, (b) chitosan-precursor-treated fiber (1 wt % chitosan, 2 wt % BTCA, and 3 wt % SHP), and (c) chitosan-nanoparticle-treated fiber (1 wt % chitosan, 2 wt % BTCA, and 3 wt % SHP).

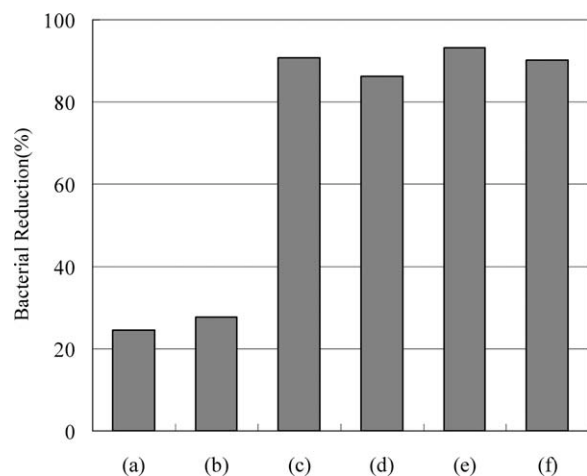


Figure 5 Bacterial reduction of *A. pernyi* silk fabrics: (a) untreated fabric before 20 launderings, (b) untreated fabric after 20 launderings, (c) fabric treated with the chitosan precursor before 20 launderings, (d) fabric treated with the chitosan precursor after 20 launderings, (e) fabric treated with nanochitosan before 20 launderings, and (f) fabric treated with nanochitosan after 20 launderings.

nanochitosan against *S. aureus* were more than 90%, even after 20 launderings. On the other hand, the chitosan nanoparticle treatment also improved the breaking strength and the wrinkle-resistance properties of the finished fabrics. However, the disadvantage for the finished fabrics treated with the nanochitosan dispersion solution was that the treatment resulted in yellowness in the fabrics.

References

1. Tsukada, M.; Goto, Y.; Freddi, G.; Matsumura, M.; Shiozaki, H.; Ishikawa, H. *J Appl Polym Sci* 1992, 44, 2203.
2. Freddi, G.; Kato, H.; Tsukada, M.; Allara, G.; Shiozaki, H. *J Appl Polym Sci* 1995, 55, 481.
3. Tsukada, M.; Arai, T.; Winkler, S. *J Appl Polym Sci* 2000, 78, 382.
4. Taddei, P.; Monti, P.; Freddi, G.; Arai, T.; Tsukada, M. *J Mol Struct* 2003, 651, 433.
5. Peng, Q.; Xu, Q.; Sun, D. F.; Shao, Z. Z. *J Appl Polym Sci* 2006, 100, 1299.
6. Gupta, D.; Haile, A. *Carbohydr Polym* 2007, 69, 164.
7. Lin, H.; Yao, L. R.; Chen, Y. Y.; Wang, H. *Fiber Polym* 2008, 9, 113.
8. Juang, R. S.; Wu, F. C.; Tseng, R. L. *Bioresour Technol* 2001, 80, 187.
9. Aguillo, E.; Rodríguez, M. S.; Ramos, V.; Albertengo, L. *Macromol Biosci* 2003, 3, 521.
10. Denkbaz, E. B.; Kilicay, E.; Birlikseven, C.; Ozturk, E. *React Funct Polym* 2002, 50, 225.
11. Kittinaovarat, S.; Kantuptim, P.; Singhaboonponp, T. *J Appl Polym Sci* 2006, 100, 1372.
12. El-Tahlawy, K. F.; El-Bendary, M. A.; Elhendawy, A. G.; Hudson, S. M. *Carbohydr Polym* 2005, 60, 421.
13. Jiong, Y. J.; Cha, S. Y.; Yu, W. R.; Park, W. H. *Text Res J* 2002, 72, 70.
14. Shin, Y.; Yoo, D. I. *J Appl Polym Sci* 1998, 67, 1515.
15. Corsi, K.; Chellat, F.; Yahia, L.; Fernandes, J. C. *Biomaterials* 2003, 24, 1255.
16. Pan, Y.; Li, Y. J.; Zhao, H. Y.; Zheng, J. M.; Xu, H.; Wei, G.; Hao, J. S.; Cui, F. D. *Int J Pharm* 2002, 249, 139.
17. Shin, Y.; Yoo, D. I.; Jang, J. *J Appl Polym Sci* 2001, 80, 2495.
18. Lu, Y. H.; Lin, H.; Chen, Y. Y.; Wang, C.; Hua, Y. R. *Fiber Polym* 2007, 8, 1.
19. Zhang, J. B. *Dye Finish* 1999, 5, 47.
20. Ye, W. J.; Leung, M. F.; Xin, J.; Kwong, T. L.; Lee, D. K. L.; Li, P. *Polymer* 2005, 46, 10538.
21. Khaled, F. E.; Magda, A. E.; Adel, G. E.; Samuel, M. H. *Carbohydr Polym* 2005, 60, 429.
22. Tang, Z. X.; Qian, J. Q.; Shi, L. E. *Mater Lett* 2007, 61, 38.
23. Kim, J. H.; Kim, Y. S.; Kim, S.; Park, J. H.; Kim, K.; Choi, K.; Chung, H.; Jeong, S. Y.; Park, R. W.; Kim, I. S.; Kwon, I. C. *J Controlled Release* 2006, 111, 231.
24. Vorkapic, D.; Matsoukas, T. *Colloid Interface Sci* 1999, 214, 283.
25. Shanta, R. B.; Remant, B. K. C.; Santosh, A.; Myung, S. K.; Hak, Y. K. *Carbohydr Polym* 2007, 69, 471.
26. Xu, X. J.; Gu, Y. *J Text Res* 2007, 28, 19.